Ethiopian Journal of Water Science and Technology (EJWST)

DOI: https://doi.org/10.59122/18519g6

Vol. 7 , 2024, Pages: 33~53 ISSN(Print): 2220-7643

Analysis of Precipitation Variability at Kulfo River Watershed: Insights from Wavelet Analysis and Back-Trajectory Approaches

Tesfay Mekonnen Weldegerima

Faculty of Meteorology and Hydrology, Water Technology Institute, Arba Minch University, Arba Minch, Ethiopia
Email: tesfaym270@gmail.com

Abstract

Understanding temporal variations and source of precipitations is essential for effective water management and flood risk mitigations, especially in regions prone to heavy precipitation events such as the Kulfo watershed. This study aims to investigate the heavy precipitation patterns at Kulfo River Watershed using wavelet analysis and an advanced atmospheric model to identify temporal precipitation characteristics and trace moisture source regions. Daily precipitation data from 1991-2020 were collected from Ethiopian Meteorology Institute. Meteorological fields on a three-dimensional grid at 1^o x 1^o spatial resolution and daily temporal resolution were also obtained from Global Data Assimilation System (GDAS). Wavelet analysis of the daily precipitation processed with the lag-1 coefficient revealed high power recurrence once every 38 to 60 days at greater than 95% confidence for red noise. The analysis also identified inter-annual periodicity in the periods_ 2002 - 2005 and 2017 - 2019. Back trajectory analysis for 3-day periods up to a heavy precipitation day during the main and short rain seasons indicated the Indian Ocean and Gulf of Eden sources. Trajectories crossed the southern and eastern African escarpment to arrive at the Kulfo watershed. Atmospheric flows associated with the Western Indian monsoon redirected by the low-level Somali winds and Arabian ridge were responsible for the moisture supply. The spatial distribution of relative humidity (RH) during heavy precipitation events ranged from 50% to 88%. The findings indicated that the time-localization of the wavelet power spectrum yielded valuable hydrological information and the back-trajectory approaches provided useful characterization of air mass sources and pathways.

Keywords: extreme precipitation events, HYSPLIT Model, moisture source, power spectrum, Kulfo Watershed

Received: 05 August, 2024; Accepted 10 September, 2024 Published: December, 2024

1. INTRODUCTION

Precipitation is a critical hydroclimatic variable whose spatial and temporal variability can significantly impact human health and livelihoods. Extremes in precipitation, such as droughts and floods, are directly linked to prolonged deficits or surpluses in precipitation. Heavy precipitation events can particularly cause extreme runoff that could damage the human and environmental systems (Knapp et al., 2008; Yisehak et al., 2020). Moreover, studies imply that the occurrence of heavy precipitations will likely increase under climate change. The Intergovernmental Panel on Climate Change Reinman, (2012) reports showed that there had been a more significant increase in the occurrences of heavy precipitations as compared to a significant decrease in many regions of the world. The report also stated that the frequency of heavy precipitation events would increase in many parts of the world in the 21st century.

Another study by Scoccimarro et al., (2013) projected increasing precipitation events over India, Southeast Asia, Indonesia, and central Africa during boreal summer, as well as over southern parts of Africa and South America during boreal winter. Some of the previous studies of extreme precipitation events in Africa indicated that climate change could bring long dry seasons and short rainy seasons. In the East African region, the results of precipitation events by different researchers were inconsistent. For example, Ogega et al., (2020) projected that the number of consecutive dry days would increase while that of wet days would decrease. However, the United Nations Office for Coordination of Humanitarian Affairs OCHA, (2019), reported around 280 people might have died owing to flooding caused by heavy precipitations in 2019 in the region. Similarly, Wainwright et al., (2021) stated that in East Africa the 2019 October –December (OND) heavy rains were registered as one of the wettest seasons in recent decades.

In Ethiopia, different patterns of precipitation have been observed at different spatiotemporal resolutions in recent decades. However, most of the studies were found to have inconsistent results. For example, studies on recent changes in precipitation amount and rainy days in Ethiopia by Seleshi & Zanke, (2004) found no significant trends. Similarly, Mekasha et al., (2014) found no significant trends of extreme precipitation from their study of 11 meteorological stations at three Ethiopian Eco environments. On the other hand, studies by Funk et al., (2012), reported a slightly increasing trend of heavy precipitations in southern and southeastern Ethiopia. Many studies were

conducted on the mean and extreme events of precipitation in and around Southern Ethiopia (Kebede & Bewket, 2009). These studies reveal mostly the trends in the past and upcoming recent decades. Hence, most of these studies were limited to assessing trends and changes in precipitation and variability, including extreme events. However, the analyses covers low spatial and temporal resolutions and consider only the main rainy seasons.

However, extreme precipitation events such as heavy precipitations occur at fine spatial and temporal resolutions from hours to a day and from a single station to small watershed levels. Moreover, the periodic nature of precipitation and the possible moisture source for heavy precipitations remained unrevealed by these studies. During July and August 2020, wide spread flooding affected several zones in Southern Ethiopia including Dawuro, Goffa, Gurage Hadya, Keffa, Silte, and South Omo zones, causing significant disruptions to livelihoods, infrastructure and agricultural activities in the region (OCHA, 2020). These recent occurrences have sparked worries and as a result of global climate change. Heavy precipitations will occur more frequently throughout the 21st century (Trenberth, 2011). Prolonged and intense precipitations have resulted in flooding and inundations in the Kulfo Watershed frequently, causing rivers to overflow and inundate areas along the river banks in lowland plains (Legese et al., 2020).

The main aim of this study is to analyze the temporal patterns of heavy precipitation events and identify their associated moisture sources in the Kulfo Watershed, using daily precipitation data from 1991 to 2020 obtained from ground based hydrometeorological stations within the study watershed. The analysis included statistical summaries, wavelet, and backward trajectory tracers. While the statistical descriptions showed the general patterns of temporal precipitations in the area, the wavelet analysis revealed the temporal characteristics of precipitation. The backward trajectory analysis allowed to track moisture sources back in time for a heavy precipitation event and thus provided information about the transport paths involved and the corresponding relative humidity during the event day. Analysis of heavy precipitation events also had important implications for understanding rates of runoff and management of downstream flood hazards. Understanding the moisture source responsible for heavy precipitation could serve as a warning for adaptations and mitigations of climate shocks.

2. MATERIALS AND METHODS

2.1 Description of the Study Area

Kulfo Watershed is located at the central part of Ethiopian Rift Valley lakes basin, between 37º18`E–37º38`E longitudes and 5º55`N–6º16`N latitudes (Figure 1). The watershed covers an area of about 500 km^2 (Wankie, 2015). Elevation of the catchment ranges from 1235 m to 3547 m above the mean sea level (Temesgen et al., 2023). Kulfo River is one of the dominant rivers in the Abaya–Chamo sub basin system (Mena et al., 2024). It originates from Guge Mountain, flowing towards the east into Lake Chamo. The river serves as a potential source of water supply to the urban and rural communities.

The climate of Kulfo Watershed is classified in the range between tropical to alpine because of its great difference in altitude and topographical elevation. The yearlong precipitation varies from 750 mm in the dry lowlands near Arba Minch town to 2342 mm in the mountainous regions of Gerese, with an average annual precipitation of 1049 mm, and mean annual temperature fluctuating between 23.05º C and 25.87ºC (Ayana et al, 2022). The precipitation distribution is bimodal with the main rainy season occurring from March to May and the second small rainy season from September to November (Mark, 2014). The watershed has an average slope of 16% and is covered dominantly by Cambisol and Regosol soil types. Besides, the soil type is characterized by shallow, moderate to deep, and very deep in depth and sandy clay to clay texture. As a result, severe land degradation resulting from soil erosion, flooding, sediment, and other materials are evident at Chamo Lake (Blumberg & Schütt, 2004). The major land use activity in the area is agriculture. However, agricultural productivity is limited owing to the frequent flood events associated with the heavy precipitations in the area

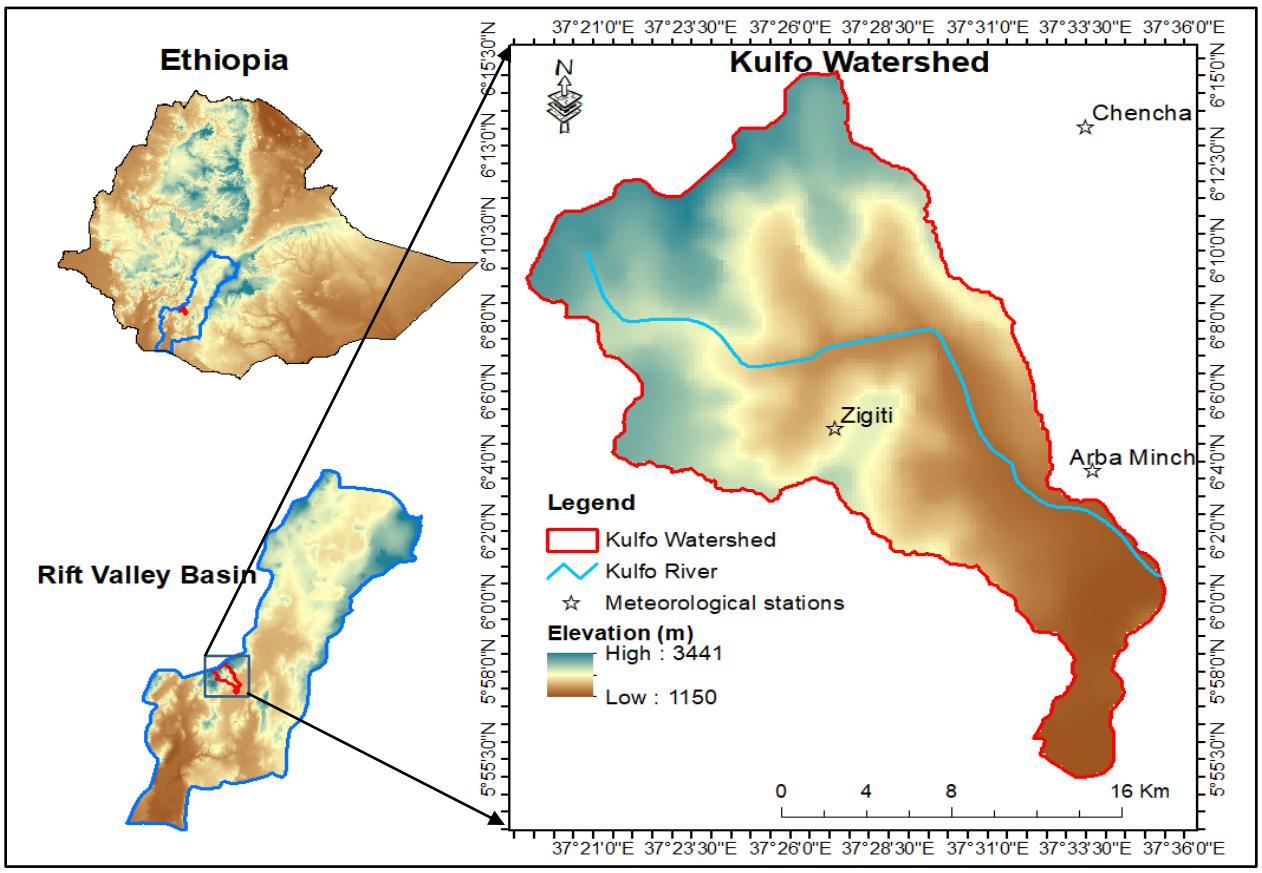

Figure 1. Geographical location of the Kulfo watershed

2.2 Data

Precipitation data of the Kulfo Watershed was collected from the Ethiopian Meteorological Institute (EMI) from 1991 to 2020 at a daily time step. The meteorological stations used for this study covers long-range records, less discontinuity, and are contributing stations to the precipitation of the study watershed. The normal ratio method was used to fill the missing values of the daily time series. The method is widely used to estimate missing values at a station by using data from nearby stations and weighted based on their long term means (Singh & Woolhiser, 2003). Before analyzing the wavelets and moisture source trajectory, the cumulative distribution function of daily precipitation was computed. The different cumulative frequency classes of the daily precipitation were calculated based on the World Meteorological Organization classifications (WMO, 2012). Table 1 illustrates the WMO standard precipitation intensity classifications. And, the precipitation days in the Kulfo Watershed from 1991-2020 are presented in Figure 2. Similarly, the very heavy precipitation days that occurred in the watershed are described in Table 2.

The other precipitation dataset was drawn from meteorological fields on a three-dimensional grid obtained from the Global Data Assimilation System (GDAS). These data sets were available at different spatial and temporal resolutions (Stein et al., 2015). The present study used the 1° × 1° spatial resolution and daily temporal resolution atmospheric fields. By utilizing the GDAS dataset with the specified spatial and temporal resolutions, the study aims to analyze and trace the trajectory of low-level atmospheric flow from a height of 10 meters above the ground at Kulfo Watershed. This information could be valuable in understanding the movement and behavior of precipitation patterns in the study area, shedding light on how meteorological conditions contribute to precipitation at Kulfo Watershed.

Table 1. Classification of precipitation intensity based on the World Meteorological Organization

Precipitation event	Precipitation (Rf) intensity in mm/day
Tiny rain	Rf < 1
Light rain	1 < Rf < 2
Low moderate rain	2 < Rf < 5
High moderate rain	5 < Rf < 10
Heavy rain	10 < Rf < 50
Violent rain	Rf > 50

Table 2. Very heavy precipitation days and amount of Precipitation (R) recorded in mm/day at Kulfo Watershed between 1991 and 2020

Precipitation date			R	Precipitation date			R	Precipitation date			R
Year	Month	Day		Precipitation date	Month	Day		Precipitation date	Month	Day	
1991	8	23	54	**2007**	9	11	67.9	**2015**	4	25	60.5
1992	6	24	71.2	**2008**	9	11	80.8		5	6	55.2
	9	23	50.1		9	24	58.7		10	19	53.7
1993	5	22	40	**2010**	5	9	71.5		11	7	60.7
1997	4	24	68.2	**2011**	5	19	64.5		12	6	54.4
1999	10	13	75.3	**2012**	4	23	59	**2016**	4	26	58
2000	5	5	54.3		4	26	50.8		6	17	56
2005	4	23	102.4		9	4	59.7		11	27	57.7
	5	14	60	**2013**	4	9	55.2	**2017**	4	27	61.3
2006	2	19	51.5		10	15	86.2	**2020**	8	31	68
	6	3	66								

2.3 Wavelet analysis

Wavelet analysis in the present study deals with the localization of the one-dimensional precipitation time series data into two-dimensional time and frequency signals. This helps to get information on both the amplitude of any periodic signals within the time series, and how this amplitude varies with time and depicts the evolution of scales and frequencies with time. The frequency analysis is more of identifying frequency domain of the time series than depicting some hydrological event occurrence for a particular return period. Wavelet analysis methods have functions capable of localizing time and frequency while decomposing several scales in the time series.

In the present study the wavelet analysis procedure is adapted from (Chan, 2000). Hence, a wavelet transform can be defined as an integral convolution of a signal S(t) with respect to the family of functions (daughters) which are derived by stretching or compressing the analyzing wavelet (mother wavelet).

$$\psi_{b,a}(t) = \frac{1}{a^{\frac{1}{2}}}\psi\left(\frac{t-b}{a}\right) \quad (1)$$

Where ψ, is the mother wavelet;

a is scale parameter;

b is position parameter

The scale or dilation parameter is always >0 however, the value is less <1 when the wavelet is dilated in the frequency direction and contracted in the time direction. The reverse condition happens when the scale value is >1. The translation and dilation process are done for each signal at every point throughout the time series.

The continuous wavelet transform is defined as the integral sum of the real signal and the scaled (compressed or dilated) signal. Continuous wavelet transform provides a smooth translation of wavelet power in terms of different wavelet coefficients from the analyzed signal of discrete time series (Torrence & Compo, 1998). In the present study, the continuous wavelet transform for the discrete precipitation time series is equated as,

$$W(b,a) = \frac{1}{(a)^{1/2}}\int \psi^{\star}\left(\frac{t-b}{a}\right)s(t)dt, \quad (2)$$

Where $\psi^{\star}$ is the complex conjugate of ψ

From equation 2, we can calculate different wavelet coefficients and scale averages at different scale values between the start and end dates of the time series. The choice of scales in orthogonal transform is limited to discrete numbers. However, in this study, a none orthogonal wavelet analysis which use a range of arbitrary scales for the Morlet wavelet is applied as suggested by (Torrence & Compo, 1998). The time series can be worked out from 1D precipitation time series into 2D data of wavelet amplitude and phase.

$$s_j = s_0 2^{j\delta j},\ j = 0,1,\dots,J \quad and, \quad J = \delta j^{-1}\log_2(N\delta t/s_0) \tag{3}$$

In this equation, s_o and J are the smallest and the largest possible scale values, respectively. The minimum scale parameter s_o is selected to approximate the equivalent Fourier period to form a time series of $2\delta t$, while Nδt is the total length of the time series. The number of sub-octaves in an octave δj is a positive value with a maximum of 0.5 sampling proportion in scale. Thus, the smaller the value of δj the finer would be the resolution of the wavelet spectrum. To minimize errors at the beginning and end of the wavelet power spectrum, the edges must be padded with sufficient zeros. This padded region, also called the cone of influence, is important in considering edge effects. On the other hand, the amplitude around the edges is discontinuous owing to the zeros filled and represented by the crosshatched regions.

A region that exceeds a 95% confidence interval is drawn for the null hypothesis of the wavelet power spectrum to show if a peak power spectrum of the time series is significantly above the background power spectrum which is the red noise spectrum.

The time averaged wavelet power over the period of the entire time series can be presented by the global power spectrum. This helps us to get information from the time-frequency distributions about how the power changes with time. The global wavelet power, $\bar{W}^2 s(b,a)$, over the entire time series s(t), can be estimated as:

$$\bar{W}^2 s(b,a) = \frac{1}{N}\sum_{b=0}^{N-1} |Ws(b,a)|^2 \tag{4}$$

2.4 Backward trajectories

The Backward trajectory analysis employed in this study is a method used to track the movement of air masses in reverse, starting from a particular location and tracing them back through time. To identify their origins and possible resources of atmospheric components such as moisture or pollutants. This study employed a three-dimensional back trajectory analysis using the Hybrid Single-Particle Lagrangian Integrated Trajectory (HYSPLIT) model version 4.8 developed by the Air Resources Laboratory (Draxler and Hess, 1998). The HYSPLIT model is a widely used atmospheric dispersion model that simulates the movement and dispersion of air parcels by integrating the equations of motion for individual particles. The model considers various atmospheric factors such as wind speed, wind direction, and atmospheric stability to calculate the trajectory of air masses.

This particular study calculated the back trajectories for three days at 10 meters above the ground level. This corresponded to a pressure level of approximately 1000 hPa above sea level. The study used a single source location and a three-dimensional velocity field to simulate the movement of the air masses backward in time. The starting time for the tracer release was set at 00 UTC. The trajectory ensemble option which starts multiple trajectories from the first selected starting location, was used in the present study form the three clustering methods.

The back-trajectory analysis allowed researchers to identify the regions from which air masses originated and tracked their movement over time (Hess et al., 1998; Stein et al., 2015). By analyzing the trajectories, the researchers determined the potential source regions for pollutants or other atmospheric constituents that cause impact on a specific location. This analysis helped to establish source-receptor relationships, which were important for understanding the transport of pollutants, assessing the impact of emissions, and studying atmospheric processes. The first position of wind advection at the start point $p(t)$ is given as:

$$p'(t + \Delta t) \quad (5)$$

Then the first and final guess positions of the trajectory can be estimated by equations (6) and (7) respectively by assuming the three-dimensional velocity vector.

$$p'(t + \Delta t) = p(t) + V(P, t)\Delta t \quad (6)$$

$$P(t + \Delta t) = P(t) + 0.5\,[V(P, t) + V(P', t + \Delta t)]\Delta t \quad (7)$$

3. RESULTS

3.1 Statistical summary of precipitation

Statistical description of the monthly seasonal and annual precipitation of the Kulfo Watershed for the period 1991-2020 is shown in Figures 2 & 3. Accordingly Figure 2 illustrates the cumulative probability distribution of the daily precipitation. Maximum precipitation was recorded in April, May, and October while minimum monthly precipitation was observed in January February, and December (Figure 3). Specifically, the highest monthly precipitation was recorded in May, but the least was observed in February. The standard deviation for the maximum precipitation was smaller than that of minimum precipitation, implying high variability during the dry months.

Similarly, the seasonal and annual precipitation patterns were analyzed (Figures not displayed). The seasonal precipitation of Kulfo Watershed showed two peaks, during the main rain season (MAM), and the second main rain season (SON). MAM received 240.4 to 575.6 mm while SON received 164.9 to 682.8 mm. The precipitation of MAM was less variable when compared to SON during the study period. On the other hand, the annual precipitation received by the area ranged from 855.1 to 1700.2 mm. However, the annual precipitation showed high annual variation of about 500 mm particularly in recent years. (Yisehak et al., 2020) described that the Kulfo Catchment received 620 to 1250 mm precipitation annually.

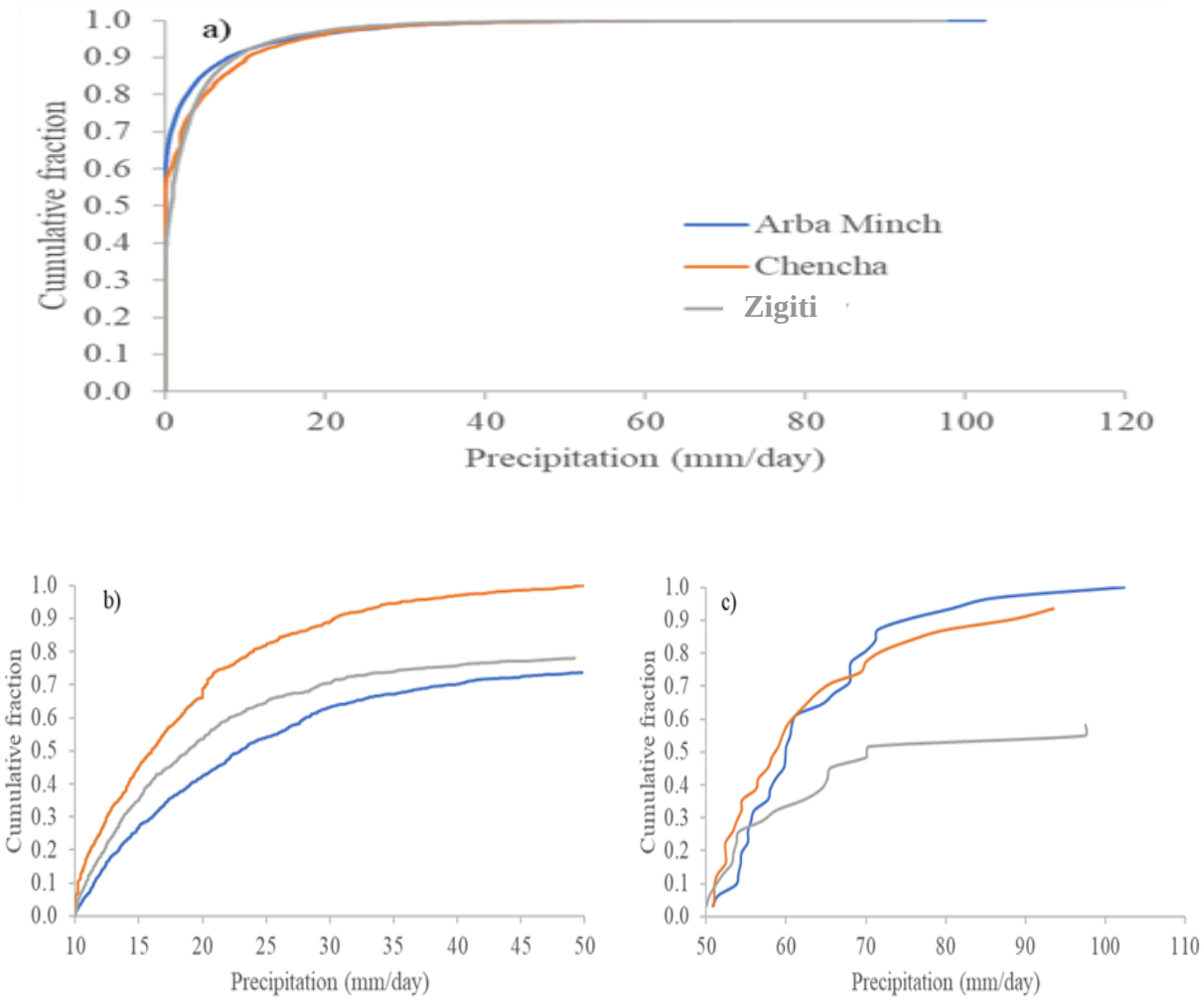

Figure 2. Cumulative distribution of daily precipitation over the Kulfo Watershed; a) All values b) Precipitations between 10 mm and 50 mm and c) Precipitations greater than 50 mm.

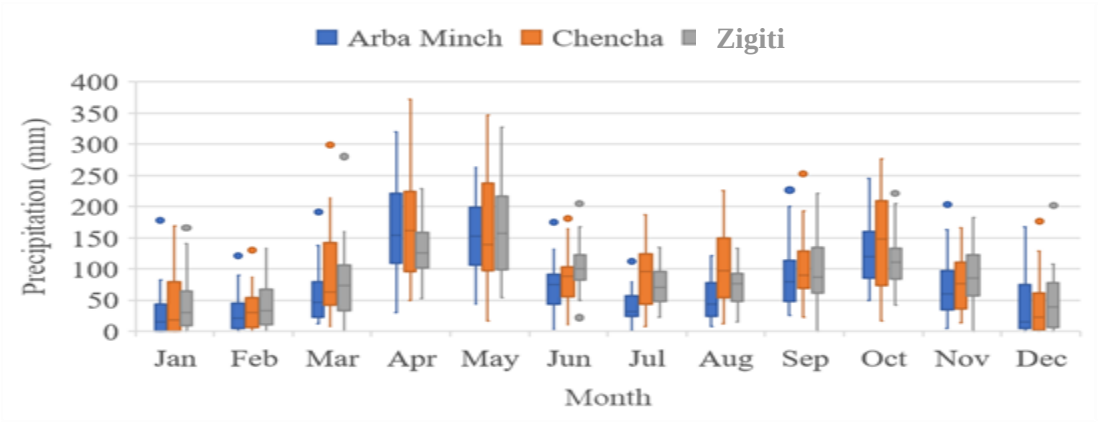

Figure 3. Box plot off Monthly precipitation over the Kulfo Watershed, 1991-2020

3.2 Wavelet Power Spectra

Figure 4 shows a plot of the daily precipitation time series for the Kulfo Watershed from 1991 to 2020 (a), the corresponding local wavelet power spectrum (b), the corresponding global wavelet spectrum (c) and its 95% confidence level for a red-noise process with a lag-1 coefficient. The concentration of power could be easily identified form the frequency or time domain in the figure.

Significant high wavelet power was observed over 32-64 months for the entire length of the record. This is illustrated by the yellow contour band located between the 32-64 months in figure 4(b). This is also illustrated by the major peak in the global wavelet spectrum figure 4(c). The other notable periods of wavelet power included 16-32, 64-128, and 128-256 months which was shown by light yellowish bands. The 16-32-month power showed high variable wavelet power for most of the record. The 64-128 months wavelet power showed oscillatory wavelet powers with high powers from 1992-1998 and 2004-2015 and lower wavelet power from 1999-2003 and 2005-2020. The scale interaction from 35-64 and 64-128 months indicated frequency modulations from early days in the year to every five year, particularly during 1992-1998 and 2004-2015. The scale-average wavelet power is a time series of the average variance in a certain band as presented in Figure 4(d). It illustrated the average of the wavelet power spectra over all scales and a measure of the average year variance over the entire time series. The semi-annual, annual, and biennial bands could be extracted by slicing the time series into corresponding scale averages; for example, 2–8 months for semiannual, 6–12 months for annual, and 16-32 months for biannual bands. A multi-year scale cyclic variance could be seen in 2006-2011 with increasing of variance in the later years. The scale-average wavelet power was used to examine modulation of one time series by another, or modulation of one frequency by another within the same time series.

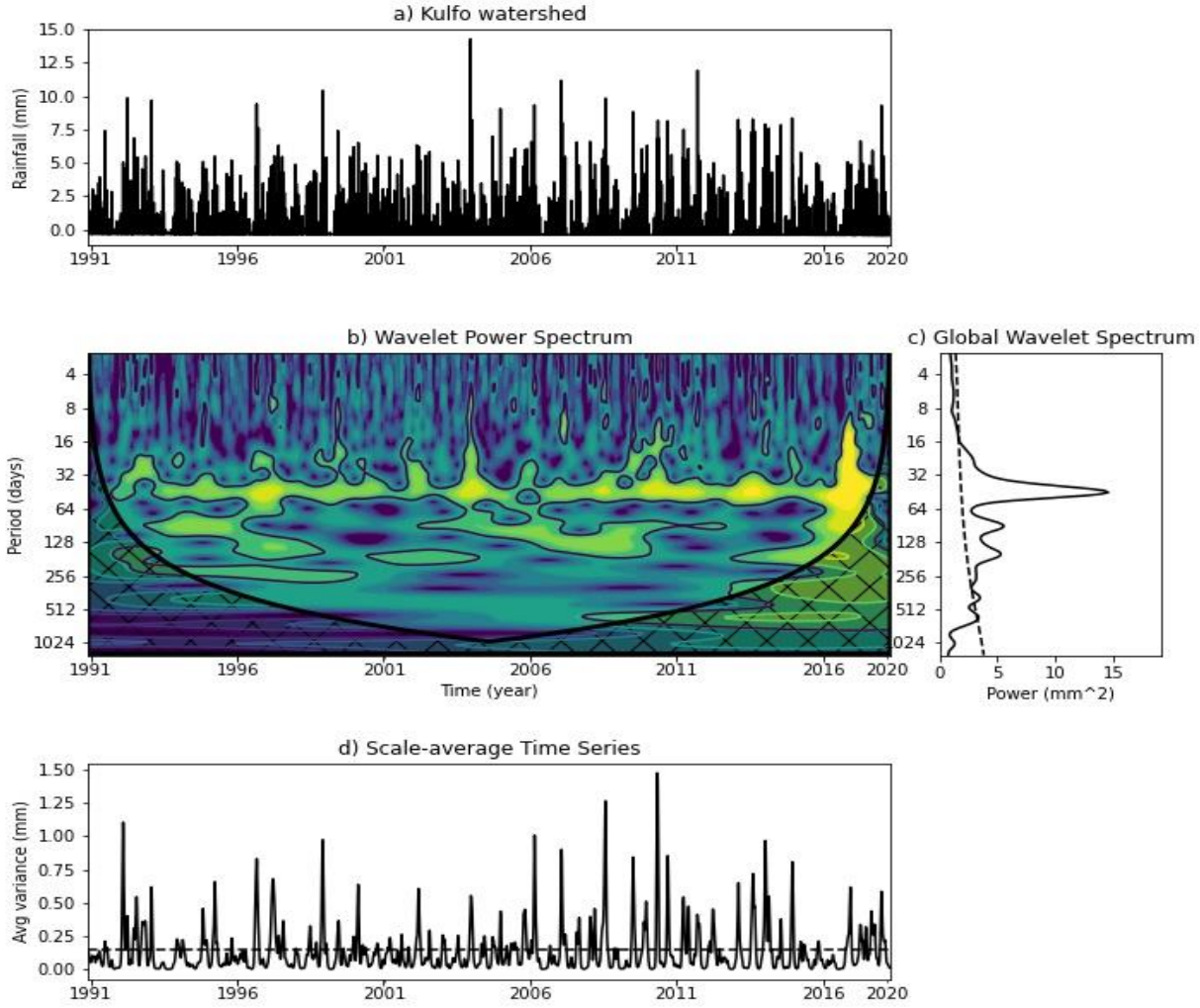

Figure 4. Wavelet spectral analysis of Kulfo Watershed for 1991-2020, (a) Normalized daily precipitation time series. (b) The wavelet power spectrum. The contour levels are chosen so that 75%, 50%, 25%, and 5% of the wavelet power is above each level, respectively. Cross-hatched region is the cone of influence, where zero padding has reduced the variance. Black contour is at 5% significance level, using a red-noise ($\alpha = 0.72$) background spectrum. (c) The global wavelet power spectrum (solid line), red noise assuming a lag-1 of a = 0.72(dashed line). (d) Scale-averaged wavelet power (solid line), 95% confidence level (dashed line).

3.3 Back-trajectories

The Backward Moisture Source Analysis is a valuable tool in atmospheric science to investigate the origins of moisture that contributes to precipitation events. The three days back-ward trajectory of moisture source paths, vertical profile, and corresponding relative humidity distribution of the

Kulfo Watershed for the two seasons is presented in this section. The analysis was performed for two extremely heavy days: one from the main rain season, 21st May 2011 and one from the short rain season, 31st October 2020. The selection of these two seasons was to assess the seasonal difference in moisture sources and paths at Kulfo Watershed. The prevailing atmospheric circulation patterns during the analysis period showed a dominant movement of moisture-laden air masses from local to regional sources.

The backward moisture source analysis for a three-day period back since 21st May 2011 was sourced from the southwest of the Indian Ocean near to Madagascar. The Indian Ocean source revealed significant insights into the moisture pathways and sources influencing precipitation in the study area. Moisture transport was dominated by distinct pathways which suggested a strong connection between the southeastern low-level flow and the moisture supply to the study area during the rainy season (Figure 5a). The relative humidity distribution showed a range of 3% to 87% across the region, indicating the presence of favorable conditions for moisture accumulation. Higher relative humidity values were observed in moisture source regions; for instance, the southwest Indian Ocean (80%) while comparatively lower values were found in areas farther away (<50%) (Figure 5b). Localized variations in relative humidity were evident because of orographic effects or the influence of local topography.

a) b)

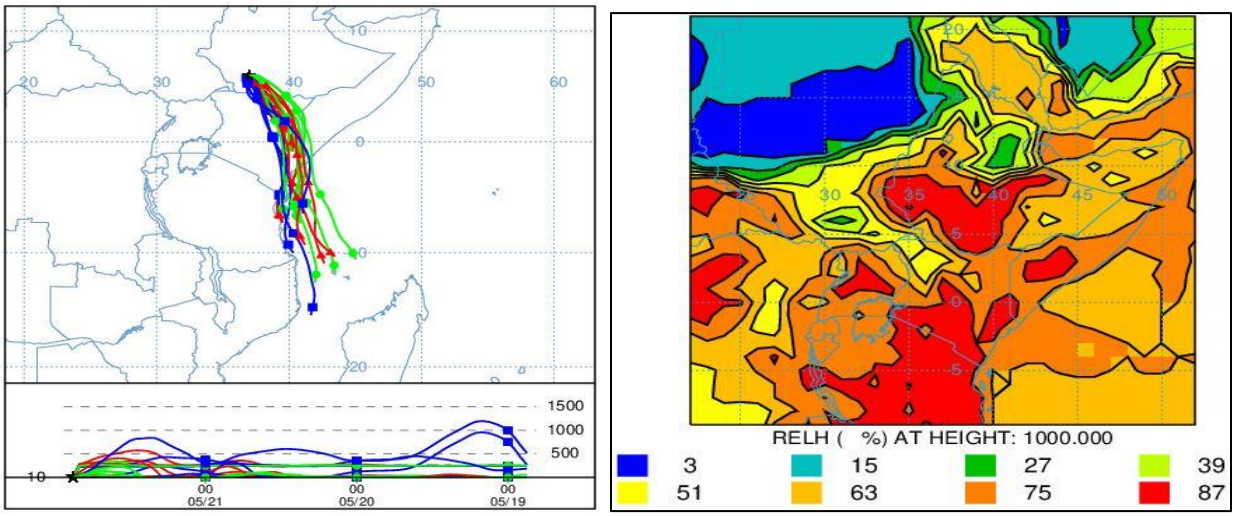

Figure 5. Back-trajectory plane view of moisture source (left) and the corresponding relative humidity (right) of the Kulfo Watershed for 21st May 2011.

The Kulfo Watershed exhibited a combination of local and remote moisture sources, each making a significant contribution to the observed precipitation. The moisture source and pathways analysis conducted for a three-day period since 31st October 2020 revealed different insights into the origins of moisture comared to 21st May 2011. The analysis indicated that the Gulf of Aden served as the primary moisture source, contributing to the moisture influx, while the southwest Indian Ocean also accounted for the moisture supply (Figure 6a). The moisture pathways exhibited a dominant flow from the Gulf of Aden towards the study region, with some local moisture-laden air masses following this trajectory. Additionally, moisture sources around the study area, such as nearby water bodies and local evapotranspiration, contributed to the overall moisture availability. These findings raised our awareness about moisture dynamics at Kulfo Watershed and provided valuable information for water resource management and forecasting in the region. Figure 6b illustrates the relative humidity distribution which ranges from 11% to 88%. This wide range indicated significant variability in moisture content across the area. The maritime influence from the Gulf of Aden caused increased humidity levels in regions closer to the coast, particularly those adjacent to the Gulf. As moist air travelledby prevailing winds, coastal and nearby areas experinced higher raltive humidity compared to locations farther away from the moisture source.

a) b)

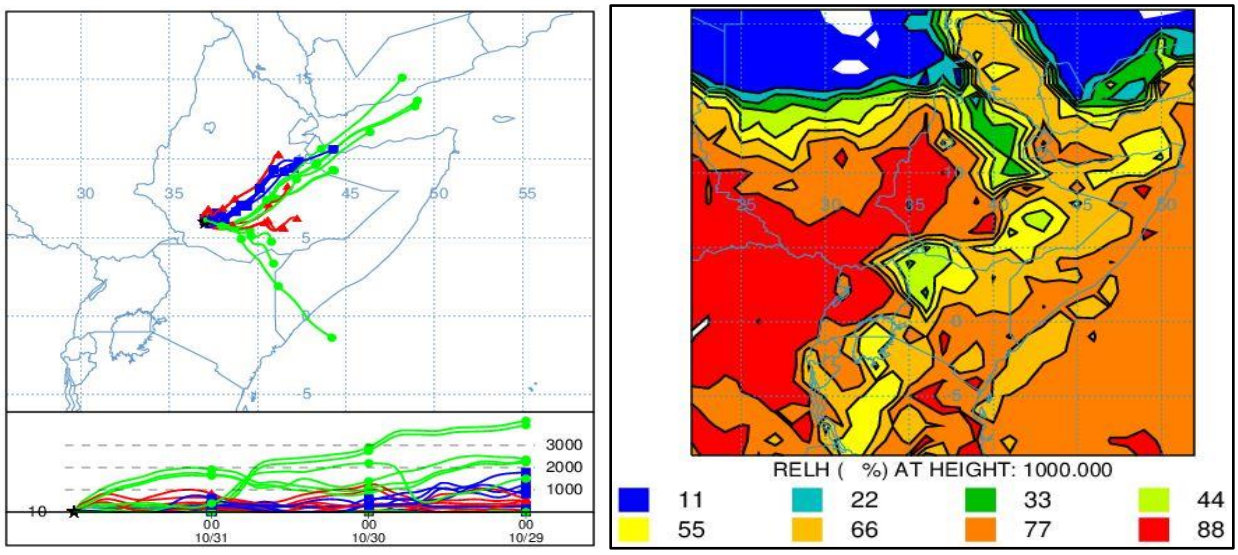

Figure 6. Back-trajectory plane view of moisture source (left) and the corresponding relative humidity (right) of the Kulfo Watershed on 31st October 2020.

4. DISCUSSIONS

The analysis of heavy precipitation events at Kulfo Watershed showed the occurrence of frequent extreme events in the watershed. The statistical summary of precipitation showed that precipitation at Kulfo Watershed was highly variable and inconsistent from month to month and from season to season. The variability was, however, relatively lower during the main rainy months (MAM) as compared to the short rain months (SON) and the other dry months. Similarly, the annual precipitation showed variability inter-annually, with the increase of wet years in the last years of the study period. (Kuma et al., 2021) reported a trend of increasing monthly precipitation in April and January at Bilate Watershed from 1981-2008. Similarly, Funk et al. (2012) found a trend of rising precipitation which was not significant in the lowlands of southern and southeastern Ethiopia.

The wavelet power spectra analysis revealed significant temporal variations in the intensity of heavy precipitation events. The results indicated dominant periodicities at multiple time scales, ranging from short-term oscillations to longer-term trends. For example, the analysis identified a significant increase in the intensity of heavy precipitation events at a decadal scale, indicating a possible influence of climate change on precipitation variability. The observed increase in heavy precipitation events aligns with previous studies conducted in southern Ethiopia. Gummadi et al., (2018), for example, indicated a statistically significant upward trend in the frequency and intensity of heavy precipitation events over the past three decades. Furthermore, (Belay et al., 2019) conducted a study on the interannual variability of precipitation in southern Ethiopia using satellite-derived datasets. The results showed the role of large-scale climate systems particularly El Niño-Southern Oscillation (ENSO) in shaping heavy precipitation patterns. Periods marked by El Niño events tended to correspond with heightened occurrences of intense precipitation across the study area.

Finally, at Kulfo Watershed the primary sources of atmospheric moisture were found to shift with the season's oceanic sources such as the Indian ocean and the Gulf of Aden. The moisture sources contributed more significantly during specific months, while continental moisture sources became more prominent during others. This seasonal variability suggested the need to account for broader regional meteorological dynamics analyzing heavy rainfall events in the area. (Dubache et al.,

2019) investigated the relationship between the Indian Ocean Dipole (IOD) and precipitation variability in southern Ethiopia. Their analysis revealed a significant correlation between positive IOD events and enhanced heavy precipitation in the study area. These results suggested that regional climate modes such as Gulf of Eden, and ENSO and IOD played a role in modulating interannual variations in heavy precipitation intensity. Moreover, the analysis of relative humidity distribution during heavy precipitation events revealed distinct spatial patterns. Regions with high relative humidity were found to be closely associated with areas exhibiting enhanced precipitation.

In addition to the seasonal and oceanic influences on moisture availability, topography, land use changes, and deforestation interacted with the atmospheric processes to shape local precipitation dynamics at Kulfo Watershed. The rugged terrain of the area enhanced orographic lifting, amplifying precipitation in elevated areas. This is particularly evident when moist air masses are funneled inland maritime sources like the Gulf of Aden. However, ongoing land use changes such as agricultural expansion, urbanization, and deforestation could significantly alter surface evapotranspiration rates, soil moisture retention, and local convective processes (Knapp et al., 2008). These landscape modifications might disrupt the local moisture recycling mechanism, potentially intensifying dry spells or exacerbating flooding events (Ayele et al., 2024). Therefore, integrating land surface characteristics with atmospheric moisture tracking approaches would be vital for designing adaptive water management strategies responsive not only to seasonal climate patterns but also to evolving land use dynamics in the region.

5. CONCLUSIONS

In this study the wavelet analysis examines the temporal variations of extreme precipitation and the backward trajectory identifies the moisture sources and pathways associated with these events. The wavelet analysis revealed significant temporal variations in the intensity of extreme precipitation events, with dominant periodicities observed at multiple time scales. The findings indicated an increase in the intensity of extreme precipitation events at a decadal scale, suggesting possible influences of long-term climate variability or climate change on precipitation patterns at Kulfo River Watershed. These results contributed to a better understanding of the dynamics and variability of extreme precipitation events in the region. The backward trajectory analysis provided insights into the moisture sources and pathways contributing to extreme precipitation events. The

analysis identified specific source regions, such as nearby oceanic or continental areas, from which moisture was transported to the study area. This information was crucial for understanding the spatio-temporal patterns of moisture transport and the associated factors driving extreme precipitation events at Kulfo River Watershed.

However, the methodologies employed in this study were not without limitations, which should be acknowledged for a balanced interpretation of the results. For example, the backward trajectory analysis helped trace moisture paths but had uncertainties due to course resolution and simplified assumptions of the GDAS model. Additionally, the complex typography of the Kulfo Watershed might introduce local atmospheric dynamics not fully captured by the trajectory model, potentially affecting the accuracy of moisture attribution. Similarly, the wavelet analysis, although effective in detecting periodicities in precipitation time series, relied on assumptions of stationarity within the segments of the signal, which might oversimplify the inherently nonlinear and chaotic nature of hydrometeorological systems.

Overall, the research highlighted the importance of investigating extreme precipitation events and their underlying mechanisms in the context of climate variability and change. The findings would contribute to the scientific understanding of extreme precipitation at Kulfo River Watershed, aiding in the development of strategies for managing and adapting to these events. Further research would be required to explore the linkages between extreme precipitation, climate drivers, and potential impacts on the local environment and society.

Acknowledgments: The author of this work is grateful to the Ethiopian Meteorological Institute (EMI) for providing the precipitation dataset.

Data availability: Data will be available up on request.

REFERENCES

Ayele, E. G., Buba, Z. M. & Garo, O. O. (2024). Evaluation of satellite rainfall products to estimate extreme flow events over the Kulfo watershed in Ethiopia. *Water Practice and Technology*, *19*(11), 4647–4666. https://doi.org/10.2166/wpt.2024.278

Belay, A. S., Fenta, A. A., Yenehun, A., Nigate, F., Tilahun, S. A., Moges, M. M., Dessie, M.,

Adgo, E., Nyssen, J. & Chen, M. (2019). Evaluation and application of multi-source satellite rainfall product CHIRPS to assess spatio-temporal rainfall variability on data-sparse western margins of Ethiopian highlands. *Remote Sensing*, *11*(22), 2688.

Blumberg, S. & Schütt, B. (2004). Character of lake floor sediments from central Lake Abaya, South Ethiopia. *Lake Abaya Research Symposium 2004-Proceedings*, *4*, 1–10.

Chan, A. (2000). Wavelet Techniques for the Analysis and Synthesis of Rainfall Data. *Journal of Water Management Modeling*, *6062*, 141–162. https://doi.org/10.14796/jwmm.r206-08

Draxler, R. R, and Hess, G. D. (1998). Description of the HYSPLIT_4 modeling system of trajectories, dispersion, and deposition. *Australian Meteorological Magazine*, *47*(1998), 295–308.

Dubache, G., Ogwang, B. A., Ongoma, V. & Towfiqul Islam, A. R. M. (2019). The effect of Indian Ocean on Ethiopian seasonal rainfall. *Meteorology and Atmospheric Physics*, *131*(6), 1753–1761.

Funk, C. C., Rowland, J., Eilerts, G., Kebebe, E., Biru, N., White, L. & Galu, G. (2012). A climate trend analysis of Ethiopia. In *Fact Sheet*. https://doi.org/10.3133/fs20123053

Gummadi, S., Rao, K. P. C., Seid, J., Legesse, G., Kadiyala, M. D. M., Takele, R., Amede, T. & Whitbread, A. (2018). Spatio-temporal variability and trends of precipitation and extreme rainfall events in Ethiopia in 1980–2010. *Theoretical and Applied Climatology*, *134*, 1315–1328.

Hess, M., Koepke, P. & Schult, I. (1998). Optical Properties of Aerosols and Clouds: The Software Package OPAC. *Bulletin of the American Meteorological Society*, *79*(5), 831–844. https://doi.org/10.1175/1520-0477(1998)079<0831:OPOAAC>2.0.CO;2

Kebede, G. & Bewket, W. (2009). Variations in rainfall and extreme event indices in the wettest part of Ethiopia. *SINET: Ethiopian Journal of Science*, *32*(2), 129–140.

Knapp, A. K., Beier, C., Briske, D. D., Classen, A. T., Luo, Y., Reichstein, M., Smith, M. D., Smith, S. D., Bell, J. E., Fay, P. A., Heisler, J. L., Leavitt, S. W., Sherry, R., Smith, B. & Weng, E. (2008). Consequences of More Extreme Precipitation Regimes for Terrestrial Ecosystems. *BioScience, 58*(9), 811–821. https://doi.org/10.1641/B580908

Kuma, H. G., Feyessa, F. F. & Demissie, T. A. (2021). Hydrologic responses to climate and land-use/land-cover changes in the Bilate catchment, southern Ethiopia. *Journal of Water*

and Climate Change, *12*(8), 3750–3769. https://doi.org/10.2166/wcc.2021.281

Legese, B., Gumi, B. & Bule Hora, E. (2020). Flooding in Ethiopia; causes, impact and coping mechanisms. A review. *International Journal of Research and Analytical Reviews*, *7*(3), 707–717.

Mark, R. J. (2014). Southern Ethiopia Rift Valley lake fluctuations and climate. *Scientific Research and Essays*, *9*(18), 794–805. https://doi.org/10.5897/sre2014.6062

Mekasha, A., Tesfaye, K. & Duncan, A. J. (2014). Trends in daily observed temperature and precipitation extremes over three Ethiopian eco-environments. *International Journal of Climatology*, *34*(6), 1990–1999. https://doi.org/https://doi.org/10.1002/joc.3816

Mena, N. B., Ayele, E. G., Chora, H. G. & Dada, T. T. (2024). Assessing the effect of rating curve uncertainty in streamflow simulation on Kulfo watershed, Southern Ethiopia. *Journal of Water and Climate Change*, *15*(9), 4199–4219. https://doi.org/10.2166/wcc.2024.645

OCHA. (2019). Ethiopia humanitarian needs overview 2019. *Relief Web*, *Feb 2019*, 8.

OCHA. (2020). *Ethiopia: 2020 kiremt weather outlook, Floods Update No.3 as Of 18 August 2020* . *3*, 1–5.

Ogega, O. M., Gyampoh, B. A. & Mistry, M. N. (2020). Intraseasonal precipitation variability over West Africa under 1.5 °c and 2.0 °c global warming scenarios: Results from cordex RCMS. *Climate*, *8*(12), 1–19. https://doi.org/10.3390/cli8120143

World Meteorological Organization, WMO (2012). Chapter 14. Observation of present and past weather; state of the ground. In *Guide to Meteorological Instruments and Methods of Observation* (pp. I–14). WMO Geneva, Switzerland.

Reinman, S. L. (2012). Intergovernmental Panel on Climate Change (IPCC). *Reference Reviews*, *26*(2), 41–42. https://doi.org/10.1108/09504121211205250

Scoccimarro, E., Gualdi, S., Bellucci, A., Zampieri, M. & Navarra, A. (2013). Heavy precipitation events in a warmer climate: Results from CMIP5 models. *Journal of Climate*, *26*(20), 7902–7911. https://doi.org/10.1175/JCLI-D-12-00850.1

Seleshi, Y. & Zanke, U. (2004). Recent changes in rainfall and rainy days in Ethiopia. *International Journal of Climatology: A Journal of the Royal Meteorological Society*, *24*(8), 973–983.

Singh, V. P. & Woolhiser, D. A. (2003). Mathematical Modeling of Watershed Hydrology.

Perspectives in Civil Engineering: Commemorating the 150th Anniversary of the American Society of Civil Engineers, 345–367. https://doi.org/10.1061/(asce)1084-0699(2002)7:4(270)

Stein, A. F., Draxler, R. R., Rolph, G. D., Stunder, B. J. B., Cohen, M. D. & Ngan, F. (2015). Noaa's hysplit atmospheric transport and dispersion modeling system. *Bulletin of the American Meteorological Society*, *96*(12), 2059–2077. https://doi.org/10.1175/BAMS-D-14-00110.1

Temesgen, E., Goshime, D. W. & Akili, D. (2023). Determination of groundwater potential distribution in Kulfo-Hare watershed through integration of GIS, remote sensing, and AHP in Southern Ethiopia. *Journal of Groundwater Science and Engineering*, *11*(3), 249–262. https://doi.org/10.26599/JGSE.2023.9280021

Torrence, C. & Compo, G. P. (1998). A Practical Guide to Wavelet Analysis. *Bulletin of the American Meteorological Society*, *79*(1), 61–78. https://doi.org/10.1175/1520-0477(1998)079<0061:APGTWA>2.0.CO;2

Trenberth, K. E. (2011). Changes in precipitation with climate change. *Climate Research*, *47*(1–2), 123–138. https://doi.org/10.3354/cr00953

Wainwright, C. M., Finney, D. L., Kilavi, M., Black, E. & Marsham, J. H. (2021). Extreme rainfall in East Africa, October 2019–January 2020 and context under future climate change. *Weather*, *76*(1), 26–31. https://doi.org/10.1002/wea.3824

Wankie, T. (2015). *Assessment of Hydrologic Impacts of Land-use Change in Kulfo River Watershed Using SWAT*.

Yisehak, B., Adhena, K., Shiferaw, H., Hagos, H., Abrha, H. & Bezabh, T. (2020). Characteristics of hydrological extremes in Kulfo River of Southern Ethiopian Rift Valley Basin. *SN Applied Sciences*, *2*(7), 1–12. https://doi.org/10.1007/s42452-020-3097-1